Development/Plasticity/Repair

Neurite Outgrowth and *In Vivo* Sensory Innervation Mediated by a $Ca_V2.2$–Laminin $\beta2$ Stop Signal

Sharon B. Sann,[1] Lin Xu,[1] Hiroshi Nishimune,[2,3] Joshua R. Sanes,[3] and Nicholas C. Spitzer[1]

[1]Neurobiology Section, University of California, San Diego, La Jolla, California 92093-0357, [2]Department of Anatomy and Cell Biology, University of Kansas, Kansas City, Kansas 66160, and [3]Department of Molecular and Cellular Biology and Center for Brain Science, Harvard University, Cambridge, Massachusetts 02138

Axons and dendrites of developing neurons establish distributed innervation patterns enabling precise discrimination in sensory systems. We describe the role of the extracellular matrix molecule, laminin $\beta2$, interacting with the $Ca_V2.2$ calcium channel in establishing appropriate sensory innervation. *In vivo*, $Ca_V2.2$ is expressed on the growth cones of *Xenopus laevis* sensory neurites and laminin $\beta2$ is expressed in the skin. Culturing neurons on a laminin $\beta2$ substrate inhibits neurite outgrowth in a specific and calcium-dependent manner. Blocking signaling between laminin $\beta2$ and $Ca_V2.2$ leads to increased numbers of sensory terminals *in vivo*. These findings suggest that interactions between extracellular matrix molecules and calcium channels regulate connectivity in the developing nervous system.

Key words: **axon guidance; calcium channel; extracellular matrix; skin; growth cone; *Xenopus***

Introduction

During neuronal development, axonal and dendritic processes must distribute appropriately within target tissues. Neurite arbors efficiently innervate sensory surfaces while maintaining discrete spatial resolution in systems such as the mammalian retina (Wassle et al., 1981), the body wall of the leech and *Drosophila* (Grueber et al., 2003; Baker and Macagno, 2007), and zebrafish and *Xenopus* skin (Kitson and Roberts, 1983; Sagasti et al., 2005). In some cases, a tiled distribution is maintained by contact mediated repulsion (Emoto et al., 2004; Sagasti et al., 2005; Baker and Macagno, 2007; Hughes et al., 2007), whereas in other cases separate or additional mechanisms are involved (Grueber et al., 2003; Gallegos and Bargmann, 2004; Lin et al., 2004; Sagasti et al., 2005). These may include intrinsic limitation of neurite growth or instruction of neurite distribution by preexistent tiled patterns of extracellular matrix molecules within target tissue (Hari et al., 2004). Particularly, "stop signals" may direct termination or instruct neurites to avoid inappropriate regions.

Calcium signals play key roles in mediating growth cone extension, turning, collapse, and stopping (Spitzer, 2006). Elevations in intracellular calcium on growth cone contact with soluble guidance molecules or extracellular matrix molecules (Snow et al., 1994) lead to inhibition of growth or neurite avoidance. Calcium responses to guidance cues are mediated by a diverse repertoire of calcium channels within the growth cone that include transient receptor potential channels and voltage-gated channels (Lipscombe et al., 1988). We describe the expression and role of $Ca_V2.2$, a canonical voltage-gated calcium channel (Nowycky et al., 1985) in the growth cone of neurites innervating the skin. $Ca_V2.2$ is notable among voltage-gated calcium channels in that it is also mechanosensitive (Calabrese et al., 2002) and binds directly to the extracellular matrix molecule laminin $\beta2$ (Nishimune et al., 2004).

Laminins are heterotrimeric glycoproteins composed of an α, β, and γ chain. Currently five α, three β, and three γ chains have been identified in the mouse and human genomes. The laminin $\beta2$ chain is localized to the synaptic but not extrasynaptic regions of the basal laminas of the neuromuscular junctions (Patton et al., 1997), as well as the retina (Hunter et al., 1992a) and subplate and floorplate of the developing CNS (Hunter et al., 1992b). The laminin $\beta2$ chain is needed for proper synapse assembly (Noakes et al., 1995a) and organizes presynaptic nerve terminals through direct interactions with $Ca_V2.1$ and $Ca_V2.2$ (Nishimune et al., 2004). Furthermore, at least *in vitro*, laminin $\beta2$ acts as a stop signal for outgrowing motor axons (Porter et al., 1995).

We have tested whether the laminin $\beta2$ interactions with $Ca_V2.2$ are responsible for the laminin $\beta2$ stop signal. We show here that interactions between laminin $\beta2$ and $Ca_V2.2$ lead to inhibition of neurite outgrowth *in vitro*. This inhibition is accompanied by calcium transients in stalled growth cones. We describe a tiled expression pattern of laminin $\beta2$ in the developing skin and demonstrate that blocking the signal between $Ca_V2.2$ and laminin $\beta2$ *in vivo* leads to changes in sensory innervation of the skin.

Received Aug. 21, 2007; revised Dec. 19, 2007; accepted Jan. 16, 2008.

This work was supported by National Institutes of Health Grant RO1MH074702 (N.C.S.) and National Science Foundation and Merck fellowships to S.B.S. We thank D. K. Berg, J. Isaacson, C. Kintner, L. N. Borodinsky, C. Root, L. W. Chang, N. A. Velasquez, B. Miller, K. Marek, G. Monsalve, W. Conroy, M. Blank, J. Stubbs, X. Nicol, and J. Y. Lin for helpful discussions and technical advice. S.B.S. and N.C.S. designed the experiments. S.B.S. and L.X. conducted the experiments. H.N. and J.R.S. provided reagents and technical advice. S.B.S., H.N., J.R.S., and N.C.S. wrote this manuscript.

The authors declare no competing financial interests.

Correspondence should be addressed to Sharon B. Sann, Neurobiology Section, University of California, San Diego, 9500 Gilman Drive, La Jolla, CA 92093-0357. E-mail: ssann@ucsd.edu.

DOI:10.1523/JNEUROSCI.3828-07.2008

Copyright © 2008 Society for Neuroscience 0270-6474/08/282366-09$15.00/0

Materials and Methods

Generation and staging of embryos. Adult female *Xenopus laevis* were injected with human chorionic gonadotropin (Sigma, St. Louis, MO) and oocytes were fertilized *in vitro*. Embryos were staged according to Nieuwkoop and Faber (1967).

RT-PCR and in situ *hybridization.* RNA was isolated from the dorsal region of stage 12–30 *X. laevis* embryos using RNAqueous-4-PCR (Ambion, Austin, TX). cDNA was generated using random hexamer primers and superscript II enzyme (Invitrogen, Carlsbad, CA). $Ca_V2.2$ primers were designed from *X. tropicalis* genomic sequence by aligning it with $Ca_V2.2$ sequence from other species to determine introns and exons. Sequence accession number and forward and reverse primers for PCR were as follows: $Ca_V2.2$ (JGI TKS329692.x1), 5′GAATTCTTCACTATGACAACGTACTGTGGGCGTTGC, and 5′GGATCCAAGGCTACACTCCGACATGACCTTATCTC, respectively. The reverse transcription (RT)-PCR product was cloned into pBluescript and sequenced (University of California, San Diego Center for AIDS Research). Antisense probes for *in situ* hybridization were generated from the PCR product of $Ca_V2.2$ using the digoxigenin RNA Labeling kit (Boehringer Mannheim, Indianapolis, IN). Sense probes were used as controls. *In situ* hybridization was performed as described previously (Harland, 1991) and modified (Burger and Ribera, 1996).

Culture. Plastic culture dishes (Corning, Corning, NY) with 200 μl volume reduction rings or 10 μl microwells (Nunc, Naperville, IL) were incubated with 5 μg/ml laminin (Sigma) alone or with 200 μg/ml 20 kDa C terminus of laminin $\beta2$ leucine-arginine-glutamate (LRE) fragment solublized by linkage to maltose binding protein or a mutated version [(LRE→QRE (glutamine-arginine-glutamate)] (Nishimune et al., 2004) in PBS for 2 h. After rinsing with filtered PBS, dishes were blocked for 2 h with 30 mg/ml heat inactivated, filtered BSA. Dishes were rinsed at least five times with PBS and two times with modified Ringer's solution [MR; containing (in mM) 116 NaCl, 0.67 KCl, 1.31 $MgSO_4$, 2 $CaCl_2$, 4.6 Tris-base, pH adjusted to 7.8 with HCl]. For loop peptide experiments, cultures were incubated with 20 μM peptide corresponding to rat $Ca_V2.1$ or $Ca_V1.2$ 11th extracellular loop (Nishimune et al., 2004) for 1 h before addition of cells. Stage 15–17 neural plates were dissected in MR containing 1 mg/ml collagenase-B (Boehringer Mannheim) and then dissociated in calcium-free medium for 1 h. Dissociated cells were cultured in MR for 14–18 h, fixed, and stained for β-tubulin as described below. For experiments with conotoxin, 5 μM ω-conotoxin-GVIA (Sigma) was added 1–2 h after plating. Tubulin-positive cells were scored for presence of a neurite longer than one cell body in diameter. There was no difference in percentage of neurons extending processes between 200 and 10 μl cultures (supplemental Fig. 1, available at www.jneurosci.org as supplemental material).

Imaging. Culture dishes were coated with the laminin $\beta2$ LRE or QRE fragment. Interleaved bands of native and denatured laminin $\beta2$ were generated by placing three electron-microscopic section multislot support grids (RB-90-Ni; Electron Microscopy Sciences, Hatfield, PA) in each dish and exposing dishes to UV illumination (12–15 cm from an 8 W bulb) for 2 h (Porter et al., 1995). This procedure yields alternating 184-μm-wide bands of native and 90-μm-wide bands of denatured laminin; the boundary is clearly visualized with illumination at 442 nm. Neurons from stage 17–20 embryos plated across both native and denatured stripes rapidly extended neurites. Cells were loaded with Fluo-4 AM and imaged as growth cones approached the boundary between denatured and native laminin $\beta2$ fragments from the denatured side. Images were captured at 2 Hz on a Leica (Nussloch, Germany) SP5 confocal microscope and analyzed with Image J. An image of the grid taken at the beginning of acquisition was superimposed onto the supplemental Fluo-4 movie (available at www.jneurosci.org as supplemental material). Comparison with the grid at the end of acquisition confirmed that the dish had not moved.

Immunocytochemistry. Whole or dissected *Xenopus* embryos were fixed with 4% paraformaldehyde (PFA), 0.1% glutaraldehyde in PBS for 30 min at 4°C. For open book dissections and HNK-1 antibody whole-embryo staining, embryos were incubated in 0.5% Triton X-100 PBS for 1–5 d before dissection or staining. Embryos were then dissected by making a ventral incision and removing the gut, notochord and myotomes to reveal the ventral surface of the neural tube and the internal surface of the skin. Cultured neurons were fixed in 4% PFA, 0.1% glutaraldehyde for 5 min. All preparations were blocked with 2% bovine serum albumin in 0.1% Triton X-100 in PBS before staining overnight at 4°C at the following concentrations: rabbit anti-$Ca_V2.2$ (Alomone, Jerusalem, Israel), 1:200; mouse IgG anti β-tubulin (Sigma), 1:500; mouse IgM anti-HNK-1 (Sigma), 1:100; mouse IgG anti-laminin $\beta2$ C4 (Hunter et al., 1989), 1:500; mouse IgM anti-laminin $\beta2$ D79, 1:10. HNK-1 whole-embryo staining was incubated at 4°C for 1–5 d. Alexa-Fluor secondary antibodies (Invitrogen) were used at 1:300 for 1–2 h at room temperature. Dissected embryos were mounted in 80% glycerol and whole-mount HNK-1-stained embryos were dehydrated in methanol and mounted in 2:1 benzyl benzoate:benzyl alcohol for clearing. Other preparations were visualized in PBS. Images of dissected embryos were acquired on a Bio-Rad (Hercules, CA) MRC-1024 confocal attachment on an Olympus (Tokyo, Japan) BX-50WI microscope. Whole-mount embryos and cultured cells were imaged with a Zeiss (Oberkochen, Germany) Axiocam MRm camera on an Axioskop 2 microscope using a 20× Achroplan water-immersion objective (whole mount and some cultures) or a Plan 10× objective (microwell cultures). *Z*-stacks of whole-mount HNK-1-stained embryos were deconvolved using the nearest neighbor algorithm on AxioVision.

Bead implants. One to two hundred mesh Affigel Blue beads (Bio-Rad) were soaked overnight in 10 μM ω-conotoxin GVIA (Sigma) in bead buffer [20 nM Na citrate, 150 mM NaCl, 1 mM $Mg(OAc)_2$, 20% glycerol, 0.02% CHAPS (3-[(3-cholamidopropyl)dimethylammonio]-1-propanesulfonate]) or 1 mg/ml calcium channel loop peptides in PBS. Beads were implanted in stage 16–18 embryos. Embryos were fixed and stained at stages 34–36.

Analysis. Cultured neurons stained with tubulin were scored for presence of a neurite longer than the diameter of the cell body. Length was measured using AxioVision software. Statistical analyses were ANOVAs followed by Dunnett's multiple comparison test against the laminin 111 control. *In vivo* images are through-series projections of the *z*-stacks of images that were used to capture the skin of the curved embryo. Quantification was done by examining slices of the *z*-stacks. A nerve terminal cluster was defined by the presence of two or more HNK-1-stained puncta in the plane of the skin and within three diameters of each other. Objectivity was assured because quantification was done blind to experimental condition. Analyses were ANOVAs followed by Tukey's multiple comparison test between all pairs of conditions. All tests were two sided. Descriptive statistics are reported as mean ± SEM.

Results

Expression and localization of $Ca_V2.2$

Calcium signaling is important for many aspects of early neuronal development, including neuronal proliferation and migration, specification of neurotransmitter phenotype, and axon guidance (Spitzer, 2006). These observations prompted us to ask what other neuronal phenotypes are regulated by early forms of calcium-dependent activity. We therefore screened candidate genes encoding calcium-permeable channels and receptors that could contribute to early excitability because of their expression patterns at early stages of development. From this screen we found that the *Xenopus* homolog of $Ca_V2.2$ was detected by RT-PCR beginning at the time of neural plate formation (stage 13) until the time of synapse formation (stage 30) (Fig. 1*A*). $Ca_V2.2$ mRNA continued to be detected until the swimming tadpole stage (stage 48) (data not shown). *In situ* hybridization with a 272 bp fragment of $Ca_V2.2$ revealed expression in the spinal cord and hindbrain beginning at the time of neural tube closure (Fig. 1*B*), leading us to pursue further investigation of this channel.

To localize $Ca_V2.2$ we immunostained whole mount preparations (Fig. 1*C*). Tailbud (stage 26) *Xenopus* embryos were stained for the neuronal marker HNK-1, revealing longitudinal tracts running anteroposteriorly, commissural axons crossing the ven-

tral midline, and sensory Rohon-Beard axons traversing the skin. Costaining with an antibody to $Ca_V2.2$ revealed expression in growth cones of extending commissural and Rohon-Beard sensory axons (Fig. 1*D–F*). Expression was also seen in the growth cones of the longitudinal tracts and growth cones initially emerging from the spinal cord (supplemental Fig. 2, available at www.jneurosci.org as supplemental material). Similarly, $Ca_V2.2$ is expressed in over 90% of growth cones of spinal neurons grown *in vitro*, specifically along the distal margin of the lamellipodia and in the filopodia (Fig. 1*G*,*H*). Expression of $Ca_V2.2$ in the growth cone suggested that it may participate in developmental growth decisions such as initiation, outgrowth, guidance, and stopping.

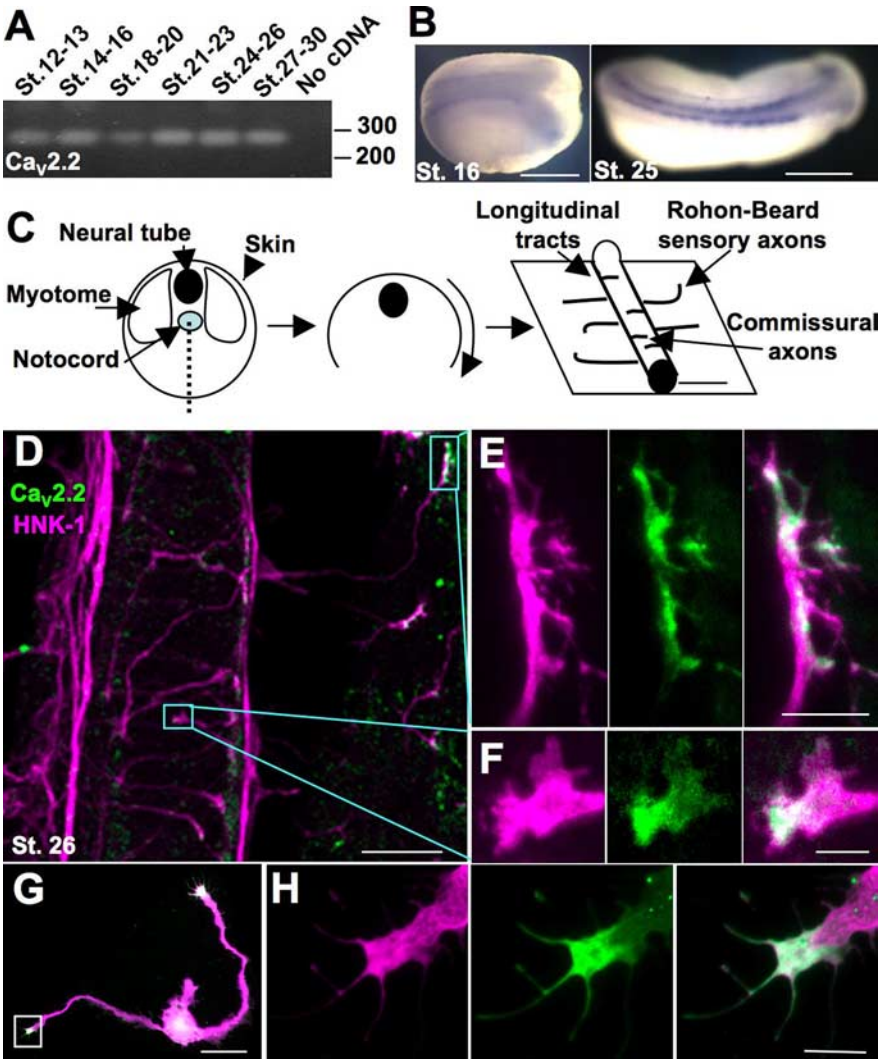

Figure 1. $Ca_V2.2$ is expressed in the developing *Xenopus* neural tube and is localized to the growth cone during axon outgrowth *in vivo* and *in vitro*. ***A***, RT-PCR of a 272 base pair fragment of $Ca_V2.2$ using mRNA collected from dissections of dorsal halves of embryos from stages (St.) 12–30. ***B***, *In situ* hybridization using the probe made from the same fragment reveals expression of $Ca_V2.2$ in the developing neural tube. Scale bar, 500 μm. ***C***, Schematized dissection for immunostaining: a ventral incision was made to remove the myotomes and notochord and reveal the neural tube and skin. Staining with the neuronal marker HNK-1 reveals longitudinal tracts running anteroposteriorly, axons of sensory Rohon-Beard neurons innervating the skin, and commissural interneurons crossing the ventral midline. ***D***, Ventral view of a spinal cord and skin of a dissected embryo stained for HNK-1 (purple) and $Ca_V2.2$ (green). Boxes outline the $Ca_V2.2$-positive growth cones pictured in ***E*** and ***F***. Scale bar, 50 μm. ***E***, Sensory Rohon-Beard growth cone expressing $Ca_V2.2$ (green). Scale bar, 10 μm. ***F***, Commissural interneuron expressing $Ca_V2.2$ (green). Scale bar, 5 μm. ***G***, Cultured neuron stained for β-tubulin (purple) and $Ca_V2.2$ (green) expressing $Ca_V2.2$ in the growth cone. Scale bar, 50 μm. ***H***, Growth cone boxed in ***G***. Scale bar, 10 μm.

Expression and localization of laminin $\beta2$

Peripheral processes of sensory neurons in *Xenopus* and other organisms innervate the skin in a distributed, tiled manner (Kitson and Roberts, 1983; Emoto et al., 2004; Gallegos and Bargmann, 2004). In some cases, tiled patterns may be specified from external guidance cues, such as stop signals that limit neurite growth. Laminin $\beta2$ has been shown to act as a stop signal for neurites of developing motor neurons (Porter et al., 1995). Because laminin $\beta2$ interacts directly with $Ca_V2.2$ (Nishimune et al., 2004), we investigated its expression in *Xenopus* skin.

Xenopus skin is composed of two layers. The inner sensorial layer gives rise to precursor cells that intercalate into the superficial layer and differentiate into ciliated cells and intercalating nonciliated cells also termed conical cells. The superficial layer contains hexagonal mucus-secreting epidermal cells as well as the ciliated cells and intercalating nonciliated cells (Fig. 2*A*) (Somasekhar and Nordlander, 1997; Stubbs et al., 2006). Immunostaining 2-d-old larvae (stage 35) with monoclonal antibodies to laminin $\beta2$ revealed association with specific cell types. Regions defined by the hexagonal cells express laminin $\beta2$, whereas regions around ciliated cells and intercalating nonciliated (or conical) cells do not express laminin $\beta2$. Similar results were obtained with two monoclonal antibodies, C4 (Fig. 2*B*) and D79 (data not shown), which recognize distinct epitopes of laminin $\beta2$.

$Ca_V2.2$ interaction with laminin $\beta2$ in culture

Because $Ca_V2.2$ and laminin $\beta2$ bind directly to each other (Nishimune et al., 2004) and are expressed where they may interact *in vivo*, we sought to determine whether this interaction affects neurite outgrowth. The eleventh extracellular loop of $Ca_V2.2$ binds an LRE motif on laminin $\beta2$ (Nishimune et al., 2004). We grew *Xenopus* neurons *in vitro* on a substrate of laminin-111 that does not have a $\beta2$ chain, on laminin-111 plus a solublized 20 kDa C-terminal fragment of the laminin $\beta2$ chain containing the LRE, or on laminin-111 plus a point mutated (LRE→QRE) laminin $\beta2$ fragment. Neurons, identified by immunostaining for neuron-specific β-tubulin, extended significantly fewer processes on substrates containing the LRE fragment (28 ± 3%) compared with QRE (42 ± 4%) or nonlaminin $\beta2$ substrates (49 ± 2%; $n \geq 6$ embryos per condition) (Fig. 3*A–C*,*F*). These results demonstrate an effect of laminin $\beta2$ on neurite extension of *Xenopus* spinal neurons.

To test whether the inhibition of neurite outgrowth is specific to interactions between laminin $\beta2$ and $Ca_V2.2$, we incubated neuronal cultures grown on laminin-111 plus the laminin $\beta2$

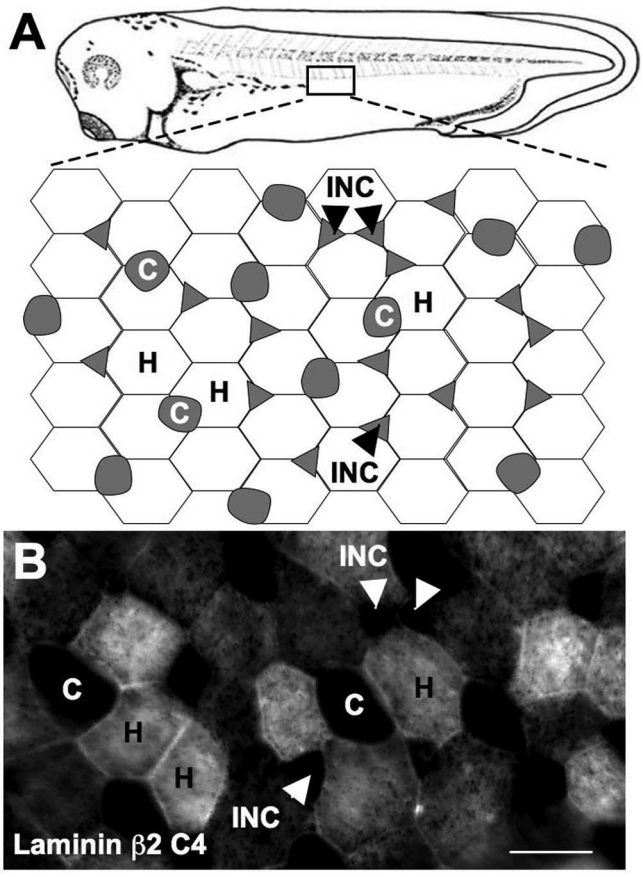

Figure 2. Laminin $\beta2$ is expressed in a tiled pattern in the skin. ***A***, Schematic of *Xenopus* skin. ***B***, Whole-embryo staining with the C4 antibody to laminin $\beta2$ revealed expression coextensive with hexagonal epithelial (H) cells but not ciliated (C) or intercalating nonciliated cells (INC) in stage 34 larvae. Scale bar, 25 μm.

LRE fragment with a peptide corresponding to the eleventh extracellular loop of rat $Ca_V2.1$. This peptide binds the LRE motif of laminin $\beta2$ (Nishimune et al., 2004) and shares 91% homology with *Xenopus* $Ca_V2.2$. As a control, we incubated cultures with the 11th extracellular loop of rat $Ca_V1.2$ that shares only 61% homology with *Xenopus* $Ca_V2.2$ (supplemental Fig. 3, available at www.jneurosci.org as supplemental material) and does not bind to laminin $\beta2$. The peptide corresponding to the 11th extracellular loop of $Ca_V2.1$ effectively rescued the inhibition by the laminin $\beta2$ LRE fragment with 50 ± 6% neurons extending processes (Fig. 3*D*,*F*). The control peptide did not rescue the inhibition by laminin $\beta2$ LRE (31 ± 3%) (Fig. 3*E*,*F*). Thus, the laminin $\beta2$ LRE inhibition is specific. Laminin $\beta2$ LRE has no effect on survival of neurons in culture, as indicated by the lack of significant differences in number of neurons per culture across conditions (data not shown).

To test whether laminin $\beta2$ inhibition of spinal neurite outgrowth is calcium-dependent, we incubated cultures grown on laminin $\beta2$ LRE in calcium-free medium or with 5 μM ω-conotoxin GVIA in standard 2 mM calcium medium. Both conditions relieve inhibition by laminin $\beta2$ LRE (45 ± 4% and 47 ± 5%, respectively) (Fig. 4) indicating that the stop signal relies on calcium influx through $Ca_V2.2$. Incubating cultures grown on laminin-111 alone in calcium-free medium does not affect the number of neurons extending processes (44 ± 6%), indicating a specific recovery of inhibition in the absence of calcium rather than a nonspecific effect of growing cultures in calcium-free medium. In addition to demonstrating the calcium dependence of laminin $\beta2$ inhibition, these results reinforce the role of $Ca_V2.2$ in laminin $\beta2$ inhibition of neurite outgrowth, because ω-conotoxin GVIA blocks $Ca_V2.2$ (Takahashi and Momiyama, 1993).

Whereas the laminin $\beta2$ LRE fragment inhibits the number of neurons that initiate processes, those neurites that have extended a process on laminin $\beta2$ are similar in length to control (supplemental Fig. 4, available at www.jneurosci.org as supplemental material) (Porter et al., 1995). We then determined whether neurites initially grown on a control substrate stall or stop when their growth cones encounter laminin $\beta2$. We generated 184-μm-wide stripes of native and 90-μm-wide stripes of UV-denatured laminin $\beta2$ LRE or QRE (Porter et al., 1995), plated neurons on them, and analyzed the behavior of growth cones migrating from denatured onto native laminin $\beta2$. We imaged intracellular calcium with Fluo-4 AM to assess calcium dynamics as growth cones palpate the border. Growth cones stalled at the LRE border generated calcium transients 10–70% above baseline fluorescence that were 1 s to 2 min in duration at half maximal amplitude and correlated with the contact of the border by one or more filopodia (Fig. 5*A*) ($n = 9$ of 9 growth cones at the border). These transients were observed at a significantly lower frequency at the QRE border (Fig. 5*B*) ($n = 2$ of 6 growth cones at the border; $p < 0.05$, Fisher's exact test). The calcium transients associated with LRE contact are distinct from the other classes of calcium transients described for these growth cones (Gu and Spitzer, 1995; Gomez et al., 2001; Conklin et al., 2005). Fifty-seven percent of growth cones stopped or turned back at the LRE border, whereas only 9% of growth cones stopped or turned at the QRE border (Fig. 5*D*) ($p < 0.0001$; $n > 80$ growth cones; Fisher's exact test).

$Ca_v2.2$–laminin $\beta2$ interactions *in vivo*

To examine the role that $Ca_V2.2$–laminin $\beta2$ interactions have in the skin *in vivo*, we first blocked signaling through $Ca_V2.2$ by implanting an agarose bead releasing ω-conotoxin GVIA into the developing embryo from the time of neural tube formation until a late larval stage (stages 16–35) when sensory terminals have been formed. This method is effective in delivering drugs that block early neuronal activity (Borodinsky et al., 2004). Using beads with fluorescently labeled ω-conotoxin, we found efficient diffusion at least 200 μm from the bead. Whole embryos were stained with HNK-1 to reveal spinal sensory neurites traversing the skin and sensory nerve terminal clusters innervating the skin. Rohon-Beard sensory axons initially run along the inner surface of the skin, continue for an undetermined length between the two layers of skin cells and form sensory varicosities in pits in the lateral or basal plasma membrane between superficial skin cells (Roberts and Hayes, 1977). The majority of these varicosities occur in clusters in an en passant manner, but some are located at nerve endings. The most heavily innervated skin cell type is the intercalating nonciliated cell (conical cell) (Somasekhar and Nordlander, 1997). Almost all nerve terminal clusters that we observe appear to form en passant as described previously by electron microscopy (Roberts and Hayes, 1977). Blocking signaling through $Ca_V2.2$ leads to a significant increase in numbers of sensory nerve terminal clusters in the skin (39 ± 8 clusters per 450×350 μm^2 area) compared with embryos in which a vehicle bead (18 ± 6) or no bead (19 ± 3) was implanted (Fig. 6).

To ask whether the effect of $Ca_V2.2$ on sensory terminals was mediated by its interaction with laminin $\beta2$, we implanted beads that release the peptide corresponding to the eleventh extracellular loop of rat $Ca_V2.1$, which blocks this interaction. These beads

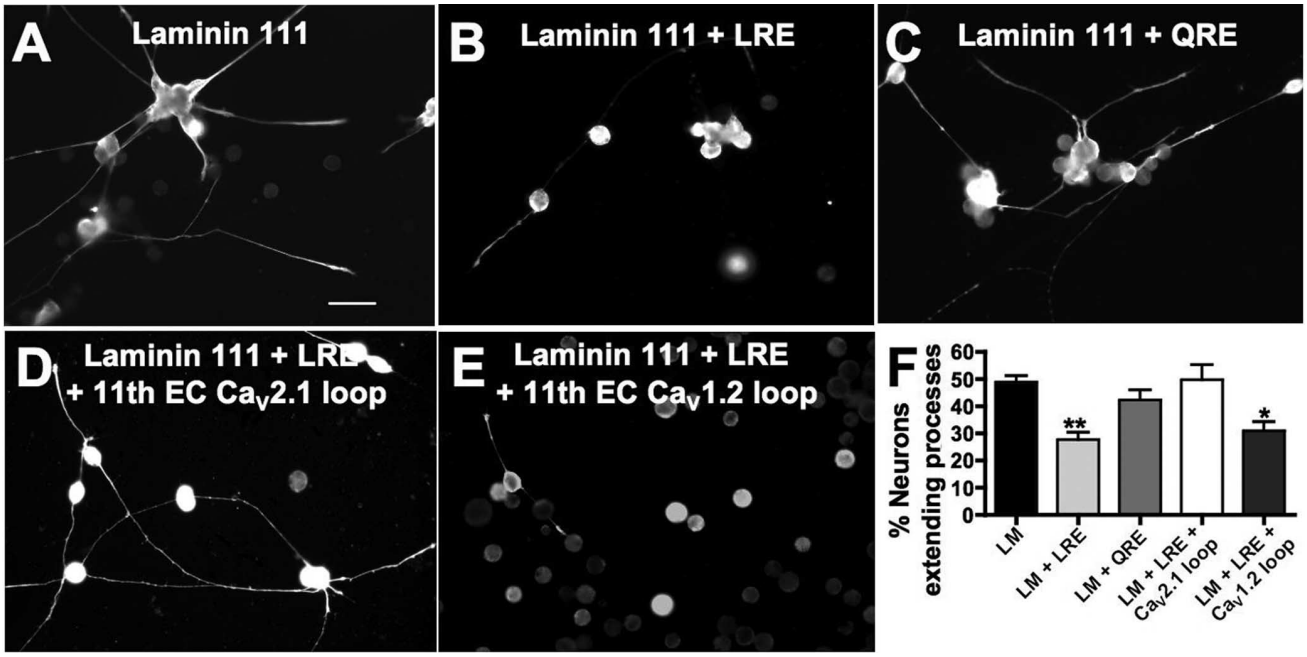

Figure 3. Laminin $\beta2$ specifically inhibits spinal neurite outgrowth. *Xenopus* neurons from stage 17 embryos were cultured on the following substrates and analyzed at 14–18 h *in vitro*: ***A***, laminin (LM) with a $\beta1$ but not a $\beta2$ chain; ***B***, a solublized 20 kDa LRE containing C-terminal fragment of laminin $\beta2$; ***C***, a point-mutated (LRE⟶QRE) laminin $\beta2$ fragment. Neurons identified by immunostaining for neuron-specific β-tubulin extended significantly fewer processes on substrates containing the LRE fragment compared with QRE or nonlaminin $\beta2$ substrates. Scale bar, 50 μm. ***D***, Incubating neurons cultured on laminin plus the $\beta2$ LRE fragment with a competing peptide corresponding to the 11th extracellular LRE-binding loop of rat $Ca_V2.1$ (91% homologous to *Xenopus* $Ca_V2.2$) rescued neurite extension. ***E***, Incubation with a control peptide corresponding to the 11th extracellular loop of rat $Ca_V1.2$ (61% homologous to *Xenopus* $Ca_V2.2$) did not prevent inhibition by laminin $\beta2$ LRE. ***F***, Laminin $\beta2$ LRE significantly reduces the number of neurons extending processes *in vitro*. This effect is rescued by incubation with the competing $Ca_V2.1$ loop peptide (**$p < 0.01$, *$p < 0.05$, comparison to LM control; $n \geq 300$ neurons from $\geq$6 cultures). Error bars indicate SEM.

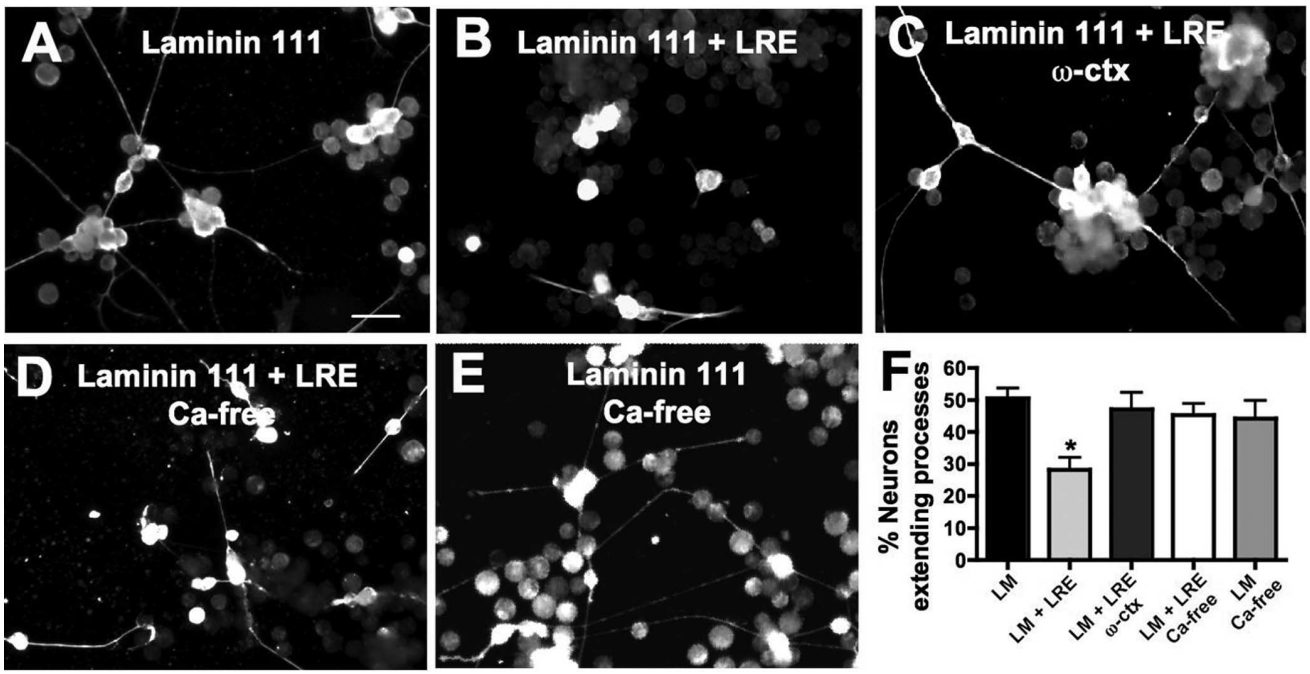

Figure 4. Laminin (LM) $\beta2$ inhibition is calcium dependent. Stage 16 dissociated neural tubes were cultured and neurons identified by staining for β-tubulin. ***A***, ***B***, Neurite outgrowth on LM is inhibited by addition of the laminin $\beta2$ fragment (LRE). Scale bar, 50 μm. ***C***, ***D***, Incubating neurons cultured on LM plus the $\beta2$ LRE fragment in 5 μM ω-conotoxin or in calcium-free medium prevents inhibition of neurite outgrowth indicating calcium dependence of LRE inhibition. ***E***, Incubating neurons grown on LM alone in calcium-free medium does not lead to increases in neurite extension. ***F***, Neurite extension on LRE is rescued by preventing calcium influx through $Ca_V2.2$ ($n \geq 250$ neurons from $\geq$7 embryos; *$p < 0.05$). Error bars indicate SEM.

resulted in significantly increased numbers of sensory nerve terminal clusters compared with embryos exposed to the control $Ca_V1.2$ loop peptide (67 ± 10 vs 36 ± 6, respectively) (Fig. 7). Although both ω-conotoxin and $Ca_V2.1$ loop-beads led to a doubling of the numbers of sensory nerve terminals in the skin, the absolute density varied in the two cases, possibly because the former were implanted during the summer and the latter during the winter; seasonal variation in amphibian development has

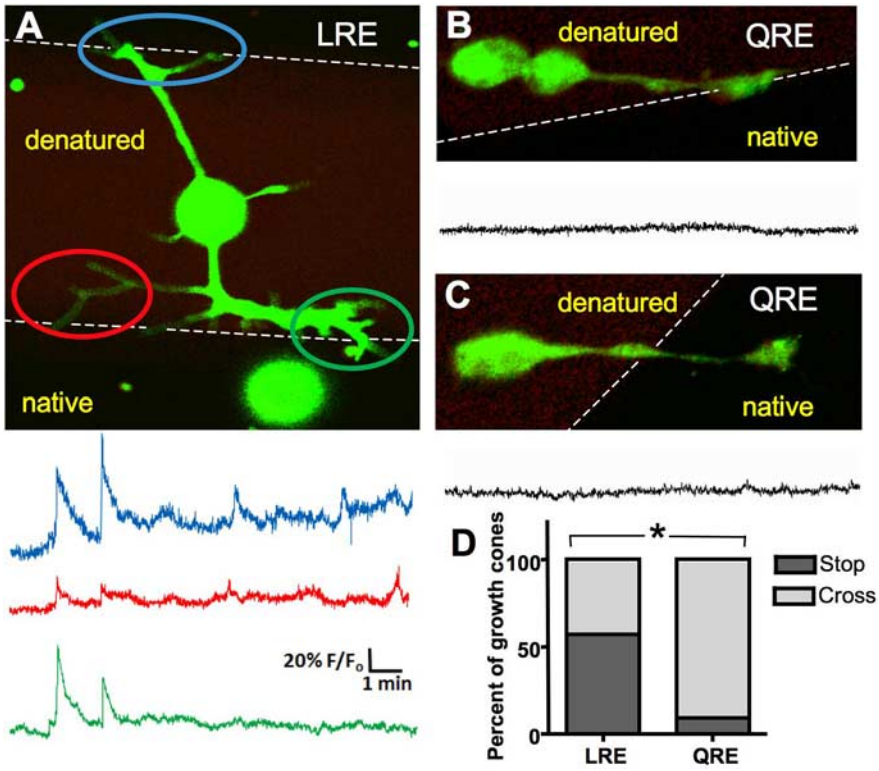

Figure 5. Neurons at a border of laminin $\beta2$ generate calcium transients and stall. ***A***, Neurons were cultured on stripes of native and UV-denatured laminin $\beta2$ LRE fragment and internal calcium concentrations were imaged using Fluo-4. Images were captured at 2 Hz. Fluo-4 is in green, denatured laminin $\beta2$ is in red, and native laminin $\beta2$ is in black. Three images were averaged to enhance visualization of the neuron. Traces show the calcium activity in each of three growth cones as they encounter the border. Axis scales apply throughout the figure. ***B***, ***C***, Less calcium transient activity is seen when a neuron approaches (***B***) or has crossed onto (***C***) activated point mutated laminin $\beta2$ (LRE⟶QRE). ***D***, Significantly more neurons stop or turn back at an LRE border than a QRE border (*$p < 0.001$).

been described previously (Wernig et al., 1980; O'Dowd et al., 1988).

Discussion

$Ca_V2.2$ is expressed in the growth cones of sensory Rohon-Beard neurons as they grow under skin cells, some of which express laminin $\beta2$. Either blocking $Ca_V2.2$ with ω-conotoxin GVIA or blocking $Ca_V2.2$–laminin $\beta2$ interactions with the $Ca_V2.1$ 11th extracellular loop leads to generation of greater numbers of sensory terminals, potentially via more en passant varicosities, greater numbers of neurites, longer neurites, or less restricted branching. These results support a model in which neurite growth and subsequent innervation are normally restricted by a calcium-dependent stop signal generated by laminin $\beta2$–$Ca_V2.2$ interactions (Fig. 8).

Specificity of laminin $\beta2$–$Ca_V2.2$ inhibition of neurite outgrowth

Previous studies have demonstrated that laminin $\beta2$ binds directly to $Ca_V2.2$ via the 11th extracellular loop of $Ca_V2.2$ and the LRE motif of laminin $\beta2$ (Sunderland et al., 2000; Nishimune et al., 2004). We present three lines of evidence indicating that these specific interactions mediate the inhibition of spinal neuron outgrowth. First, inhibition is observed when neurons are grown on a laminin $\beta2$ fragment containing the LRE motif, but not one containing the point mutated QRE. Second, inhibition is rescued when cultures are incubated with the competing peptide corresponding to the eleventh extracellular loop of $Ca_V2.2$. Finally, ω-conotoxin GVIA, a specific inhibitor of $Ca_V2.2$, blocks laminin $\beta2$-mediated inhibition. These results indicate that laminin $\beta2$ acts via $Ca_V2.2$ to inhibit neurite outgrowth. Furthermore, growing neurons on stripes of native and denatured laminin $\beta2$ LRE demonstrates that neurites already growing on a denatured laminin $\beta2$ substrate are inhibited by initial contact with an active laminin $\beta2$ substrate. This initial contact appears to be signaled through the growth cone by a calcium transient.

Calcium dependence of laminin $\beta2$–$Ca_V2.2$ inhibition of neurite outgrowth

Inhibition of neurite outgrowth by laminin $\beta2$ is blocked by incubating cultures in calcium-free medium or ω-conotoxin GVIA, demonstrating calcium dependence. Additionally Fluo-4 calcium imaging of neurons approaching a laminin $\beta2$ border reveals calcium transients on growth cone contact with laminin $\beta2$. The reliance of laminin $\beta2$–$Ca_V2.2$ inhibition on calcium influx distinguishes this effect from the role that laminin $\beta2$ plays in clustering presynaptic calcium channels and other active zone proteins in the presynaptic nerve terminal, a calcium-independent effect (Nishimune et al., 2004). The calcium dependence of laminin $\beta2$–$Ca_V2.2$ neurite inhibition raises the intriguing possibility that laminin $\beta2$ may activate $Ca_V2.2$ or $Ca_V2.1$, the other presynaptic calcium channel to which it binds. However, channel properties of $Ca_V2.1$ heterologously expressed in human embryonic kidney (HEK) cells are not changed by presentation of the laminin $\beta2$ LRE fragment (Nishimune et al., 2004). There are several mechanisms by which laminin $\beta2$ may produce a change in the calcium signal through $Ca_V2.2$ that would affect neurite outgrowth but that would be undetected in recordings from HEK cells. First, $Ca_V2.2$ and $Ca_V2.1$ may require an additional molecule not present in HEK cells to be activated by laminin $\beta2$. Second, laminin $\beta2$ may serve to cluster $Ca_V2.2$ to a microdomain in growth cones at which it can effectively transduce a calcium signal. Indeed, laminin $\beta2$ clusters $Ca_V2.1$ at the mammalian neuromuscular junction (Nishimune et al., 2004). Similar changes in distribution of $Ca_V2.2$ in HEK cells might not lead to changes in the current recorded. Third, the involvement of $Ca_V2.2$ in generating a stop signal may rely on the mechanosensitivity of this channel (Calabrese et al., 2002). The interaction of the moving growth cone expressing $Ca_V2.2$ channels with the static LRE motif of laminin $\beta2$ may constitute an adequate stimulus for channel activation that is absent from $Ca_V2.1$ expressed in nonmotile HEK cells. Indeed, calcium influx through other mechanosensitive channels within the growth cone inhibits neurite outgrowth (Jacques-Fricke et al., 2006).

Regulation of sensory innervation by laminin $\beta2$–$Ca_V2.2$ interactions

Laminin $\beta2$ functions in synapse formation at neuromuscular junctions (Hunter et al., 1989; Noakes et al., 1995a; Porter et al., 1995; Nishimune et al., 2004) in glomerular filtration in the kid-

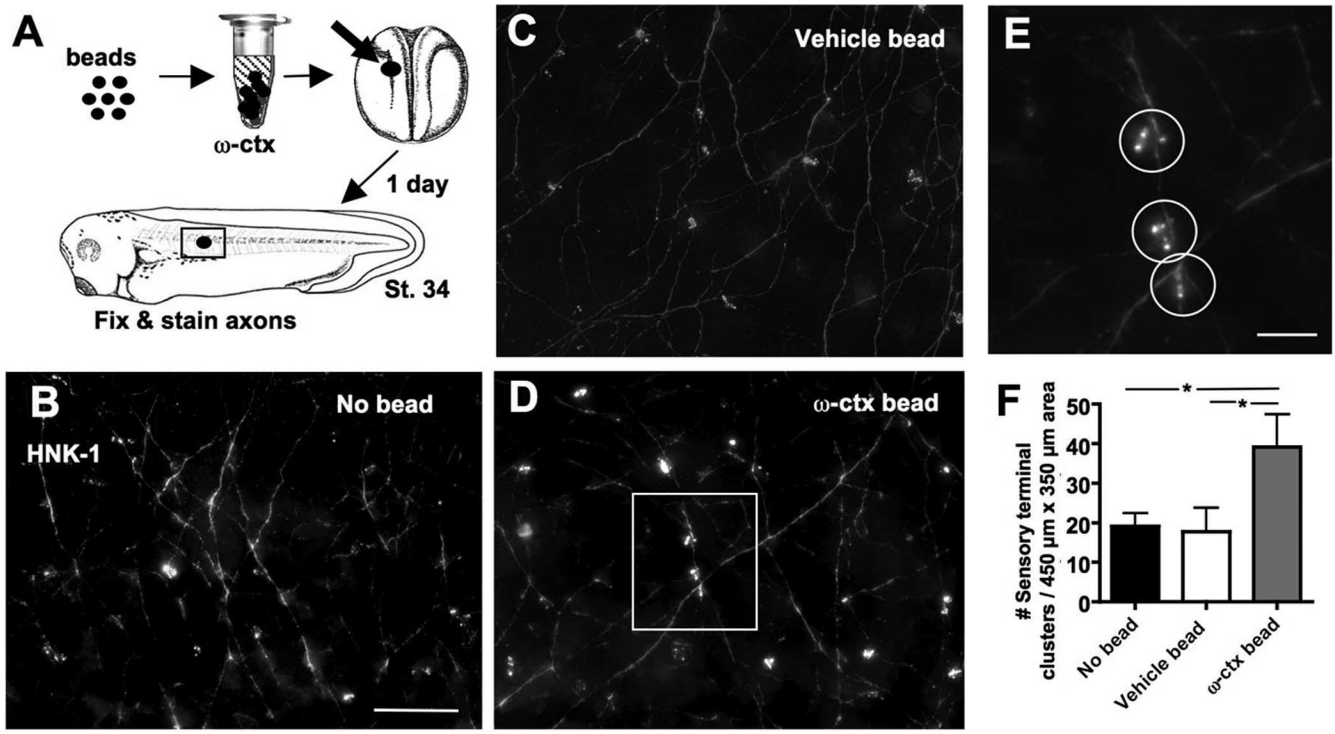

Figure 6. Blocking signaling through $Ca_V2.2$ *in vivo* leads to increased innervation of the skin. ***A***, Agarose beads soaked in 10 μM ω-conotoxin (ctx) were implanted in stage 16 embryos. After 1 d, stage 34 embryos were fixed and stained with anti-HNK-1 to reveal sensory processes and sensory nerve terminals innervating the skin. A 450 × 350 μm area centered around the bead was imaged and analyzed (box). ***B–D***, Deconvolved and projected *z*-series through the skin of embryos in which no bead (***B***), a control bead (***C***), or an ω-conotoxin bead (***D***) were implanted. Scale bar, 50 μm. ***E***, Enlarged image of the boxed region in ***D*** showing three sensory nerve terminal clusters, circles. Scale bar, 10 μm. ***F***, Embryos exposed to ω-conotoxin exhibited significantly greater numbers of sensory nerve terminal clusters compared with embryos implanted with a vehicle bead or no bead (*$p < 0.05$). Error bars indicate SEM.

ney (Noakes et al., 1995b), and in cell fate determination in the retina (Hunter et al., 1992a; Zenker et al., 2004). Here, we describe the expression of laminin $\beta2$ in the skin and its role in regulating sensory innervation. This expression is consistent with evidence for expression of human laminin $\beta2$ in embryonic dermis and epidermis (Iivanainen et al., 1995). Indeed, incorporating a mixture of laminins, including the laminin $\beta2$ chain, into skin grafts improves sensory perception achieved during regeneration (Caissie et al., 2006).

Growth of sensory neurites is mediated by neurotrophic factors such as NT-4 (Krimm et al., 2006) and guidance molecules such as ephrins (Moss et al., 2005). Branching and tiled patterning of sensory neurites relies on the NDR (nuclear Dbf2-related) kinase family in both like-repels-like tiling (Emoto et al., 2006) and noncontact-mediated distribution (Gallegos and Bargmann, 2004). We have identified a role for calcium signaling elicited by an extracellular matrix molecule in sensory neurite innervation. The activation of NDR kinases is calcium-dependent, providing a potential mechanism by which calcium influx through $Ca_V2.2$ may lead to changes in sensory innervation (Millward et al., 1998).

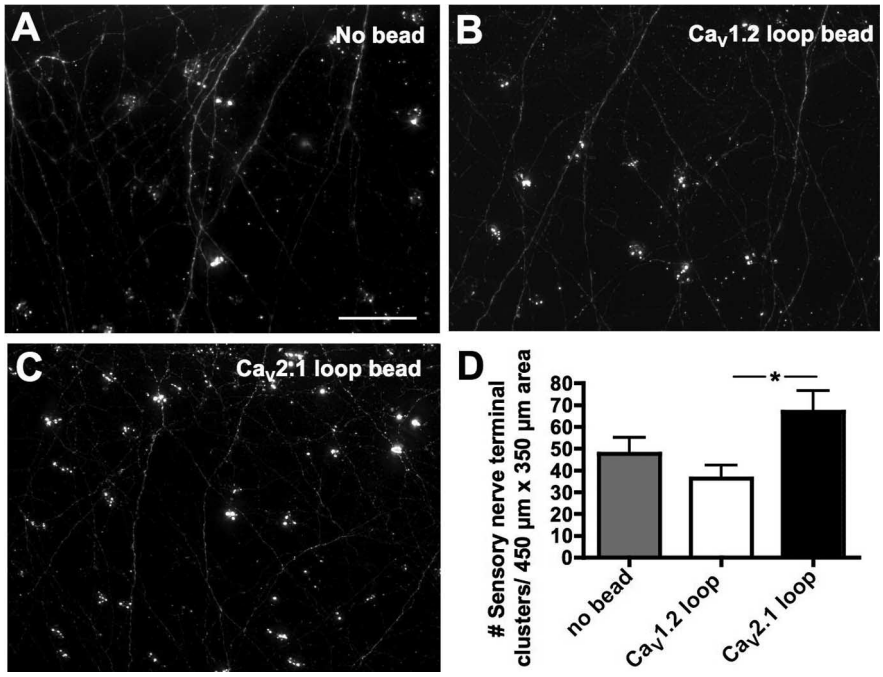

Figure 7. Blocking $Ca_V2.2$–laminin $\beta2$ interactions *in vivo* leads to increased innervation of the skin. ***A–C***, Agarose beads soaked in 10 μM $Ca_V2.1$ or $Ca_V1.2$ 11th extracellular loop peptide were implanted in stage 16 embryos. After 1 d, stage 34 embryos were fixed and stained with anti-HNK-1 to reveal sensory processes and sensory nerve terminals innervating the skin as in Figure 6. Scale bar, 50 μm. ***D***, Embryos exposed to $Ca_V2.1$ loop peptide (***C***) exhibited significantly greater numbers of sensory nerve terminals than embryos exposed to $Ca_V1.2$ loop peptide (***B***) (*$p < 0.05$; $n \geq 3$ embryos for each condition). Error bars indicate SEM.

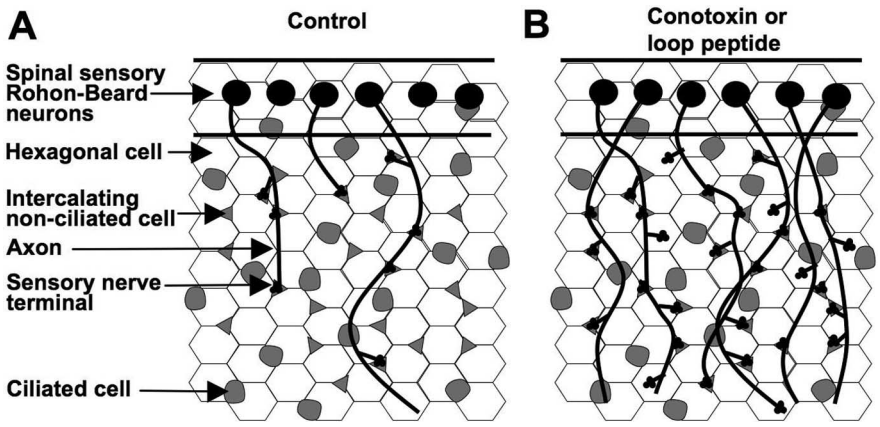

Figure 8. Model of laminin $\beta2$ and $Ca_V2.2$ interactions in development of skin innervation. ***A***, In control conditions, outgrowing sensory terminals are inhibited or slowed by laminin $\beta2$-rich regions of the skin coextensive with hexagonal cells (white). ***B***, The number of sensory nerve terminals increases when signaling interactions between laminin $\beta2$ and $Ca_V2.2$ are blocked.

Classes of stop signals

Laminin $\beta2$ has been described as a stop signal for motor neurite outgrowth (Porter et al., 1995). A stop signal may function to indicate that neurites have reached their targets where they are to form synapses or terminal endings (Becker et al., 2000; Poskanzer et al., 2003; Dimitropoulou and Bixby, 2005). Alternatively, a stop signal may inhibit a neuron from growing into nontarget regions (Manzini et al., 2006). Our results are consistent with the latter function because inhibiting the signal through $Ca_V2.2$ leads to increased numbers of sensory nerve terminals. Behaviorally, this may lead to hypersensitivity to light touch and/or mislocalization of sensory signals. Pierson syndrome, a rare human disorder caused by mutations to the *LAMB2* gene that encodes laminin $\beta2$, has been characterized by kidney failure, blindness, muscle dystonia, microcephaly, and neurological disorders (Zenker et al., 2004; Wuhl et al., 2007). It is likely that these infants would also have abnormalities in somatosensation.

Ziconotide, an inhibitor of $Ca_V2.2$ derived from conus snail venom, has recently begun to be used for pain treatment, delivered intrathecally (Lynch et al., 2006). Although the amount of this drug present in general circulation is quite low, with 56% of patients having <0.15 nM plasma levels, the IC_{50} for its inhibition of $Ca_V2.2$ heterologously expressed in *Xenopus* oocytes is 0.45 nM (Luchian, 2001). The role that we have demonstrated for $Ca_V2.2$ in axon guidance and sensory innervation during development suggests that the use of Ziconotide in breast feeding or pregnant women is ill advised. Laminin $\beta2$ is also expressed centrally in the mammalian developing cortex in the subplate (Hunter et al., 1992b), a transient population of neurons that is crucial to establishment of thalamocortical connections and maturation of inhibition (Kanold and Shatz, 2006). Ziconotide could disrupt normal innervation here as well.

References

Baker MW, Macagno ER (2007) In vivo imaging of growth cone and filopodial dynamics: evidence for contact-mediated retraction of filopodia leading to the tiling of sibling processes. J Comp Neurol 500:850–862.

Becker CG, Meyer RL, Becker T (2000) Gradients of ephrin-A2 and ephrin-A5b mRNA during retinotopic regeneration of the optic projection in adult zebrafish. J Comp Neurol 427:469–483.

Borodinsky LN, Root CM, Cronin JA, Sann SB, Gu X, Spitzer NC (2004) Activity-dependent homeostatic specification of transmitter expression in embryonic neurons. Nature 429:523–530.

Burger C, Ribera AB (1996) *Xenopus* spinal neurons express Kv2 potassium channel transcripts during embryonic development. J Neurosci 16:1412–1421.

Caissie R, Gingras M, Champigny MF, Berthod F (2006) In vivo enhancement of sensory perception recovery in a tissue-engineered skin enriched with laminin. Biomaterials 27:2988–2993.

Calabrese B, Tabarean IV, Juranka P, Morris CE (2002) Mechanosensitivity of N-type calcium channel currents. Biophys J 83:2560–2574.

Conklin MW, Lin MS, Spitzer NC (2005) Local calcium transients contribute to disappearance of pFAK, focal complex removal, and deadhesion of neuronal growth cones and fibroblasts. Dev Biol 287:201–212.

Dimitropoulou A, Bixby JL (2005) Motor neurite outgrowth is selectively inhibited by cell surface MuSK and agrin. Mol Cell Neurosci 28:292–302.

Emoto K, He Y, Ye B, Grueber WB, Adler PN, Jan LY, Jan YN (2004) Control of dendritic branching and tiling by the Tricornered-kinase/Furry signaling pathway in *Drosophila* sensory neurons. Cell 119:245–256.

Emoto K, Parrish JZ, Jan LY, Jan YN (2006) The tumour suppressor Hippo acts with the NDR kinases in dendritic tiling and maintenance. Nature 443:210–213.

Gallegos ME, Bargmann CI (2004) Mechanosensory neurite termination and tiling depend on SAX-2 and the SAX-1 kinase. Neuron 44:239–249.

Gomez TM, Robles E, Poo M, Spitzer NC (2001) Filopodial calcium transients promote substrate-dependent growth cone turning. Science 291:1983–1987.

Grueber WB, Ye B, Moore AW, Jan LY, Jan YN (2003) Dendrites of distinct classes of *Drosophila* sensory neurons show different capacities for homotypic repulsion. Curr Biol 13:618–626.

Gu X, Spitzer NC (1995) Distinct aspects of neuronal differentiation encoded by frequency of spontaneous Ca^{2+} transients. Nature 375:784–787.

Hari A, Djohar B, Skutella T, Montazeri S (2004) Neurotrophins and extracellular matrix molecules modulate sensory axon outgrowth. Int J Dev Neurosci 22:113–117.

Harland RM (1991) In situ hybridization: an improved whole-mount method for *Xenopus* embryos. Methods Cell Biol 36:685–695.

Hughes ME, Bortnick R, Tsubouchi A, Baumer P, Kondo M, Uemura T, Schmucker D (2007) Homophilic dscam interactions control complex dendrite morphogenesis. Neuron 54:417–427.

Hunter DD, Shah V, Merlie JP, Sanes JR (1989) A laminin-like adhesive protein concentrated in the synaptic cleft of the neuromuscular junction. Nature 338:229–234.

Hunter DD, Murphy MD, Olsson CV, Brunken WJ (1992a) S-laminin expression in adult and developing retinae: a potential cue for photoreceptor morphogenesis. Neuron 8:399–413.

Hunter DD, Llinas R, Ard M, Merlie JP, Sanes JR (1992b) Expression of s-laminin and laminin in the developing rat central nervous system. J Comp Neurol 323:238–251.

Iivanainen A, Vuolteenaho R, Sainio K, Eddy R, Shows TB, Sariola H, Tryggvason K (1995) The human laminin beta 2 chain (S-laminin): structure, expression in fetal tissues and chromosomal assignment of the LAMB2 gene. Matrix Biol 14:489–497.

Jacques-Fricke BT, Seow Y, Gottlieb PA, Sachs F, Gomez TM (2006) Ca^{2+} influx through mechanosensitive channels inhibits neurite outgrowth in opposition to other influx pathways and release from intracellular stores. J Neurosci 26:5656–5664.

Kanold PO, Shatz CJ (2006) Subplate neurons regulate maturation of cortical inhibition and outcome of ocular dominance plasticity. Neuron 51:627–638.

Kitson DL, Roberts A (1983) Competition during innervation of embryonic amphibian head skin. Proc R Soc Lond B Biol Sci 218:49–59.

Krimm RF, Davis BM, Noel T, Albers KM (2006) Overexpression of neurotrophin 4 in skin enhances myelinated sensory endings but does not influence sensory neuron number. J Comp Neurol 498:455–465.

Lin B, Wang SW, Masland RH (2004) Retinal ganglion cell type, size, and

spacing can be specified independent of homotypic dendritic contacts. Neuron 43:475–485.

Lipscombe D, Madison DV, Poenie M, Reuter H, Tsien RY, Tsien RW (1988) Spatial distribution of calcium channels and cytosolic calcium transients in growth cones and cell bodies of sympathetic neurons. Proc Natl Acad Sci USA 85:2398–2402.

Luchian T (2001) The influence exerted by the beta(3) subunit on MVIIA omega-conotoxin binding to neuronal N-type calcium channels. Biochim Biophys Acta 1512:329–334.

Lynch SS, Cheng CM, Yee JL (2006) Intrathecal ziconotide for refractory chronic pain. Ann Pharmacother 40:1293–1300.

Manzini MC, Ward MS, Zhang Q, Lieberman MD, Mason CA (2006) The stop signal revised: immature cerebellar granule neurons in the external germinal layer arrest pontine mossy fiber growth. J Neurosci 26:6040–6051.

Millward TA, Heizmann CW, Schafer BW, Hemmings BA (1998) Calcium regulation of Ndr protein kinase mediated by S100 calcium-binding proteins. EMBO J 17:5913–5922.

Moss A, Alvares D, Meredith-Middleton J, Robinson M, Slater R, Hunt SP, Fitzgerald M (2005) Ephrin-A4 inhibits sensory neurite outgrowth and is regulated by neonatal skin wounding. Eur J Neurosci 22:2413–2421.

Nieuwkoop PD, Faber J (1967) Normal table of *Xenopus laevis* (Daudin): a systematical and chronological survey of the development from the fertilized egg till the end of metamorphosis, Ed 2. Amsterdam: North-Holland.

Nishimune H, Sanes JR, Carlson SS (2004) A synaptic laminin-calcium channel interaction organizes active zones in motor nerve terminals. Nature 432:580–587.

Noakes PG, Gautam M, Mudd J, Sanes JR, Merlie JP (1995a) Aberrant differentiation of neuromuscular junctions in mice lacking s-laminin/laminin beta 2. Nature 374:258–262.

Noakes PG, Miner JH, Gautam M, Cunningham JM, Sanes JR, Merlie JP (1995b) The renal glomerulus of mice lacking s-laminin/laminin beta 2: nephrosis despite molecular compensation by laminin beta 1. Nat Genet 10:400–406.

Nowycky MC, Fox AP, Tsien RW (1985) Three types of neuronal calcium channel with different calcium agonist sensitivity. Nature 316:440–443.

O'Dowd DK, Ribera AB, Spitzer NC (1988) Development of voltage-dependent calcium, sodium, and potassium currents in *Xenopus* spinal neurons. J Neurosci 8:792–805.

Patton BL, Miner JH, Chiu AY, Sanes JR (1997) Distribution and function of laminins in the neuromuscular system of developing, adult, and mutant mice. J Cell Biol 139:1507–1521.

Porter BE, Weis J, Sanes JR (1995) A motoneuron-selective stop signal in the synaptic protein S-laminin. Neuron 14:549–559.

Poskanzer K, Needleman LA, Bozdagi O, Huntley GW (2003) N-cadherin regulates ingrowth and laminar targeting of thalamocortical axons. J Neurosci 23:2294–2305.

Roberts A, Hayes BP (1977) The anatomy and function of "free" nerve endings in an amphibian skin sensory system. Proc R Soc Lond B Biol Sci 196:415–429.

Sagasti A, Guido MR, Raible DW, Schier AF (2005) Repulsive interactions shape the morphologies and functional arrangement of zebrafish peripheral sensory arbors. Curr Biol 15:804–814.

Snow DM, Atkinson PB, Hassinger TD, Letourneau PC, Kater SB (1994) Chondroitin sulfate proteoglycan elevates cytoplasmic calcium in DRG neurons. Dev Biol 166:87–100.

Somasekhar T, Nordlander RH (1997) Selective early innervation of a subset of epidermal cells in *Xenopus* may be mediated by chondroitin sulfate proteoglycans. Brain Res Dev Brain Res 99:208–215.

Spitzer NC (2006) Electrical activity in early neuronal development. Nature 444:707–712.

Stubbs JL, Davidson L, Keller R, Kintner C (2006) Radial intercalation of ciliated cells during *Xenopus* skin development. Development 133:2507–2515.

Sunderland WJ, Son YJ, Miner JH, Sanes JR, Carlson SS (2000) The presynaptic calcium channel is part of a transmembrane complex linking a synaptic laminin ($\alpha4$ $\beta2$ $\gamma1$) with non-erythroid spectrin. J Neurosci 20:1009–1019.

Takahashi T, Momiyama A (1993) Different types of calcium channels mediate central synaptic transmission. Nature 366:156–158.

Wassle H, Peichl L, Boycott BB (1981) Dendritic territories of cat retinal ganglion cells. Nature 292:344–345.

Wernig A, Pecot-Dechavassine M, Stover H (1980) Sprouting and regression of the nerve at the frog neuromuscular junction in normal conditions and after prolonged paralysis with curare. J Neurocytol 9:278–303.

Wuhl E, Kogan J, Zurowska A, Matejas V, Vandevoorde RG, Aigner T, Wendler O, Lesniewska I, Bouvier R, Reis A, Weis J, Cochat P, Zenker M (2007) Neurodevelopmental deficits in Pierson (microcoria-congenital nephrosis) syndrome. Am J Med Genet A 143:311–319.

Zenker M, Aigner T, Wendler O, Tralau T, Muntefering H, Fenski R, Pitz S, Schumacher V, Royer-Pokora B, Wuhl E, Cochat P, Bouvier R, Kraus C, Mark K, Madlon H, Dotsch J, Rascher W, Maruniak-Chudek I, Lennert T, Neumann LM, et al. (2004) Human laminin beta2 deficiency causes congenital nephrosis with mesangial sclerosis and distinct eye abnormalities. Hum Mol Genet 13:2625–2632.